REPORT DOCUMENTATION PAGE

Form Approved
OMB No. 0704-0188

1. REPORT DATE (DD-MM-YYYY)	2. REPORT TYPE	3. DATES COVERED (From - To)
30-07-2012	Final Technical	01-08-2009 to 30-07-2012

4. TITLE AND SUBTITLE
Funtionalised silk fibres

5a. CONTRACT NUMBER

5b. GRANT NUMBER
FA9550-09-1-0332

5c. PROGRAM ELEMENT NUMBER

6. AUTHOR(S)
Tara Sutherland

5d. PROJECT NUMBER

5e. TASK NUMBER

5f. WORK UNIT NUMBER

7. PERFORMING ORGANIZATION NAME(S) AND ADDRESS(ES)
CSIRO Ecosystem Sciences
GPO 1700
Canberra ACT 2600
Australia

8. PERFORMING ORGANIZATION REPORT NUMBER

9. SPONSORING / MONITORING AGENCY NAME(S) AND ADDRESS(ES)
AFOSR
875 N. Randolph St
Arlington, VA 22203

10. SPONSOR/MONITOR'S ACRONYM(S)

11. SPONSOR/MONITOR'S REPORT NUMBER(S)
AFRL-OSR-VA-TR-20120921

12. DISTRIBUTION / AVAILABILITY STATEMENT
Choose one:
A = Approved for public release; distribution is unlimited

13. SUPPLEMENTARY NOTES

14. ABSTRACT

The aim of this project was to understand the structure-properties-performance relationship of honeybee silks and to use this information to guide design of second-generation honeybee silk materials. We demonstrated that solutions of a single recombinant silk protein could adopt the native silk molecular structure and mechanical properties. We selected a number of amino acids for specific alanine to cysteine mutations and then used site-directed mutagenesis followed by recombinant expression to make these mutants in E. coli. We demonstrated that mutation did not affect our ability to produce the protein at high levels, purify them to generate concentrated silk protein solutions, or our ability to fold them into the native molecular structure. These results indicate that the protein is not under strong sequence constraint and is ideally suited for development of second-generation protein materials.

15. SUBJECT TERMS

16. SECURITY CLASSIFICATION OF:			17. LIMITATION OF ABSTRACT	18. NUMBER OF PAGES	19a. NAME OF RESPONSIBLE PERSON
a. REPORT	b. ABSTRACT	c. THIS PAGE			Tara Sutherland
unclassified	unclassified	unclassified	unclassified (U)		19b. TELEPHONE NUMBER (Include area code) 61-2- 6246 4236

Standard Form 298 (Rev. 8-98)
Prescribed by ANSI Std. Z39.18

Grant Title: FUNCTIONALISED SILK FIBRES
Grant Number: FA9550-09-1-0332

Final report: July 30th 2010

Tara Sutherland

Abstract

The aim of this project was to understand the structure-properties-performance relationship of honeybee silks and to use this information to guide design of second-generation honeybee silk materials. We demonstrated that a single recombinant silk protein could adopt the native silk molecular structure and be fabricated into materials with equivalent mechanical properties to that generated from recombinant proteins produced from the four silk genes found in honeybees. We selected a number of amino acids for specific alanine to cysteine mutations and then used site-directed mutagenesis followed by recombinant expression to make these mutants in *E. coli*. We demonstrated that mutation did not affect our ability to produce the protein at high levels, purify them to generate concentrated silk protein solutions, or our ability to fold them into the native molecular structure. These results indicate that the protein is not under strong sequence constraint and is ideally suited for development of second-generation protein materials.

Another major part of this project investigated the molecular structure of native honeybee silk in more detail. We demonstrated that native silk contains beta-sheet structures as well as the previously described coil molecular structure. Although these beta-sheets are important functional components of honeybee silk, we demonstrated that the presence of beta-sheets is insufficient to explain the mechanical performance of the material, so we examined the possibility of cross-linking between protein chains in native silk. Amino acid analysis of the material demonstrated a deficiency in lysine residues in comparison to that predicted from protein sequences. Analysis of native proteins within the silk glands indicated the presence of covalent cross-links before silk fibre fabrication. Based on these results we refined the coiled coil molecular structural model of honeybee silk to include low levels of both beta-sheet and covalent cross-links. We developed a range of bio-mimetic silk materials with differing levels of beta-sheet and covalent cross-linking and demonstrated that these materials had similar structure and performance to native silks. Our refined structural model provides a template from which to design second generation silken materials.

Summary of progress towards objectives

Objective 1 – Mutagenesis: *We will choose one of the four honeybee silk proteins. Based on our structural models, we will select alanine residues in the sequence that we hypothesize are non-essential for inter-protein interactions and are located on the fibre surface. We will use oligonucleotide-directed mutagenesis systems to replace the selected alanine codons with cysteine codons.*

Objective achieved in Year 1

Objective 2 - Expression and purification of the silk protein mutants: *The mutants will be cloned into the pET14b expression vector then individually expressed in E. coli inclusion bodies. After expression under optimized conditions, inclusion bodies will be purified from this mixture and solubilised using SDS.*

Objective achieved in Year 1

Objective 3 - Verification of surface location of cysteine residues: *The purified silk protein mutants will be prepared under conditions that promote the formation of coiled coils. The amount of solvent exposed cysteine will be assessed by reaction with Ellmans reagent (5,5'-dithiobis(2-nitrobenzoate; DTNB). The product of this reaction is readily detected colorimetrically using a standard spectrophotometer.*

Objective achieved in Year 1

Objective 4 - Verification of native structure: *The mutants will be examined by circular dichroism (CD) to confirm coiled coil structure. The thermal stability of the substituted coiled coil will be compared to the stability of the native silk coiled coil.*

Objective partially achieved in Year 1 (folding of mutants into coiled coils was confirmed using FTIR) and modified in Year 2

Modified Objective 4 – Determination of factors controlling artificial silk protein folding into native structure. *The effect of SDS and salt on folding AmelF3 in solution will be examined by circular dichroism (CD) to confirm factors that promote folding of the protein into the coiled coil structure.*

Objective achieved in Years 2 and 3

Objective 5 - Synthesis of silken materials: *Mutant silk proteins will be concentrated by dialysis against commercially available protein concentrating reagents. Concentrated silk protein solutions will be fabricated into fibres by extrusion into a methanol coagulation bath, dried and then drawn to 100% their original length or by electrospinning.*

Objective achieved in Year 1 and 2

Objective 6 - Proof-of-concept functionalisation: *The availability of reactive cysteine on the surface of the silk thread will be assessed by reaction with a fluorophore such as 5-iodoacetamidofluorescein (IAF) and examination of the threads by fluorescence microscopy.*

Objective partially achieved in Year 1

Objective 7 - Physical analysis of functionalised fibres: *The tensile strength and extensibility of the functionalised fibres will be measured using an Instron Tensile tester to assess the effects of the mutagenesis on the native properties of the material.*

Objective achieved in Year 1 and 2

Objective 8 – Recursion: *If the above steps do not produce the desired results, we will refine the structural model and select alternate sites for mutagenesis.*

Objective achieved in Year 3

Detailed description of results

Objective 1 – Mutagenesis: *We will choose one of the four honeybee silk proteins. Based on our structural models, we will select alanine residues in the sequence that we hypothesize are non-essential for inter-protein interactions and are located on the fibre surface. We will use oligonucleotide-directed mutagenesis systems to replace the selected alanine codons with cysteine codons.*

Selection of silk protein. Native honeybee silk is made from four structural proteins, named AmelF1–4. The proteins are similar in length, amino acid composition and molecular architecture (Sutherland et al., 2006). All four honeybee silk proteins were expressed in *E. coli*. Recombinant AmelF3 protein, in isolation, was shown to adopt the coiled coil structure of native honeybee silk in solution (Figure 1A) and in dried films (Figure 1B). Threads generated from AmelF3 protein alone had equivalent mechanical properties to fibres generated from all four honeybee silk proteins (Table 1). As it was demonstrated that AmelF3 alone could adopt the native silk structure and achieve equivalent mechanical properties to material generated from the four orthologous honeybee silk proteins and native silk, it was chosen as the template for mutagenesis.

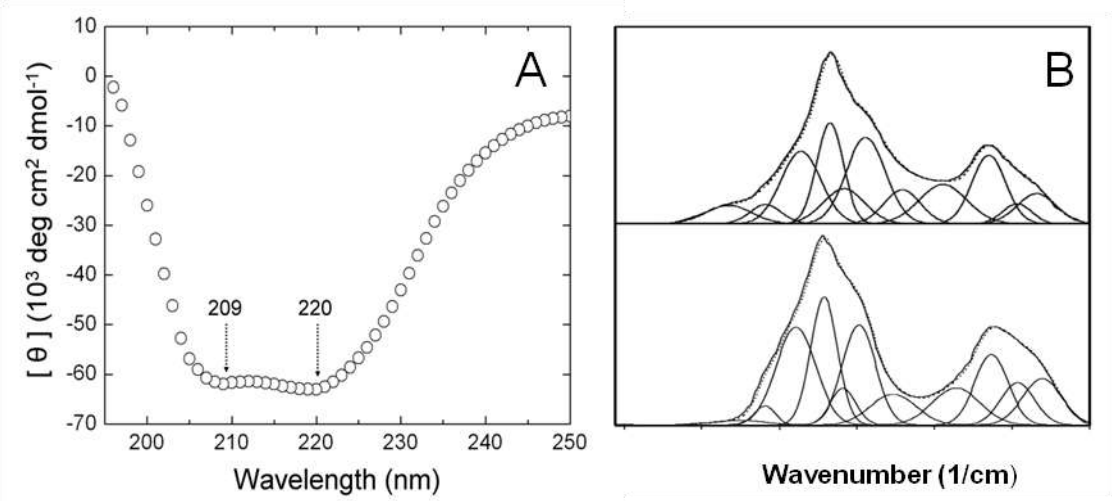

Figure 1. Structural and physical properties showing that a single honeybee silk protein has equivalent structure to native silk. (A) Circular dichroism spectrum of AmelF3 protein solution showing strong spectral minima at 220 and 209 nm, indicative of coiled coil structure (Zhou et al., 1994). (B) Fourier Transform Infrared spectroscopy (FTIR) spectra and deconvolutions of AmelF3 films (top) and native honeybee silk (bottom) with maxima in the amide I region at 1652 cm^{-1} and 1629 cm^{-1}, consistent with a coiled coil structure (Heimburg et al., 1999).

Table 1. Mechanical properties of AmelF3 honeybee silk fibers, in comparison to fibres from all four honeybee silk proteins (AmelF1-4) and native silks.

Method of fabrication	Constituent proteins	Diameter (μm)	Breaking stress (MPa)	Breaking strain (%)
Extruded into 70% MeOH	AmelF1-4	31 ± 2	70 ± 4	190 ± 11
	AmelF3	45 ± 2	50 ± 3	243 ± 10
Extruded into 70% MeOH then drawn ≈100% in 90% MeOH	AmelF1-4	21 ± 1	129 ± 11	97 ± 13
	AmelF3	34 ± 2	97 ± 7	129 ± 15
Extruded into 70% MeOH then drawn ≈300% in 90% MeOH	AmelF1-4	17 ± 1	203 ± 10	51 ± 5
	AmelF3	23 ± 1	178 ± 20	68 ± 9
Natural[1]	*Native*	*9*	*132*	*204*

[1]Hepburn et al., 1979

Selection of residues for mutagenesis. A set of alanine to cysteine mutations at amino acids 75, 192-198 and 257 (Figure 2) were designed based on the structural model described in Sutherland et al. (2006). Coiled coils are characterised by a seven-residue heptad repeating sequence of amino acid character, with the first and fourth residues being generally more hydrophobic than the other residues. The AmelF3 A to C mutations encompassed each position in one of the classic coiled coil heptad repeats. In addition, a residue at either end of the coiled coil region and in predicted non-core positions were chosen for mutagenesis.

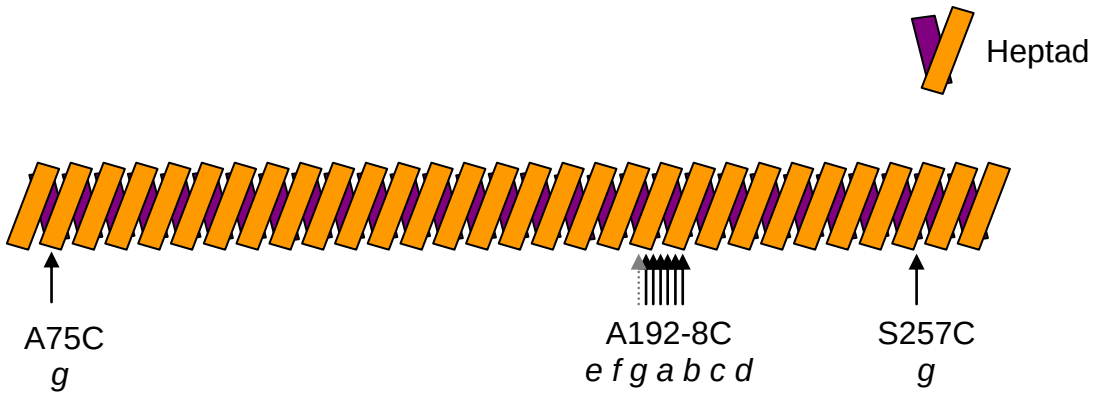

Figure 2. Schematic showing relative position of alanine (A) to cysteine (C) mutagenesis sites selected within the 210 coiled coil region of AmelF3.

Objective 2 - Expression and purification of the silk protein mutants: *The mutants will be cloned into the pET14b expression vector then individually expressed in E. coli inclusion bodies. After expression under optimized conditions, inclusion bodies will be purified from this mixture and solubilised using SDS.*

The mutations described in Objective 1 were created using the Gene Tailor Site-Directed Mutagenesis protocol from Invitrogen. The mutants were sequenced to verify that the mutation had occurred and then protein expression in *E. coli* was optimised for each mutation. Eight of the nine mutants could be expressed at levels equivalent to the native AmelF3 constructs (Figure 3 top). The proteins could be readily purified from inclusion bodies to high levels of purity and concentration using BugBuster Master Mix (Novagen) according to the manufacturer's protocol (Figure 3 middle). Silk proteins were solubilised in 3% sodium dodecyl sulfate (SDS) with 2 h incubation at 60 °C and stored at 4 °C until required. The silk protein purity was checked by SDS-PAGE electrophoresis and protein concentration determined using the BCA method (Sigma, St Louis).

Under reducing conditions, the proteins ran as monomers during SDS-PAGE (Figure 3 middle) and the hydrodynamic diameter of the mutants, determined by dynamic light scattering, was 9.2 +/- 0.1 nm—the expected size for monomeric proteins. Under non-reducing conditions, it is expected that the cysteine residues will form disulfide linkages with the equivalent residue on a single adjacent protein. As expected all the mutants ran as dimers under non-reducing conditions (Figure 3 bottom), and the hydrodynamic diameter of particles in the protein solution was measured at 10.7 +/- 0.2 nm—the size expected if the volume of the protein particles doubled as the result of dimerisation of the proteins through disulfide linkages. These results confirm the presence of cysteine residues in the mutants.

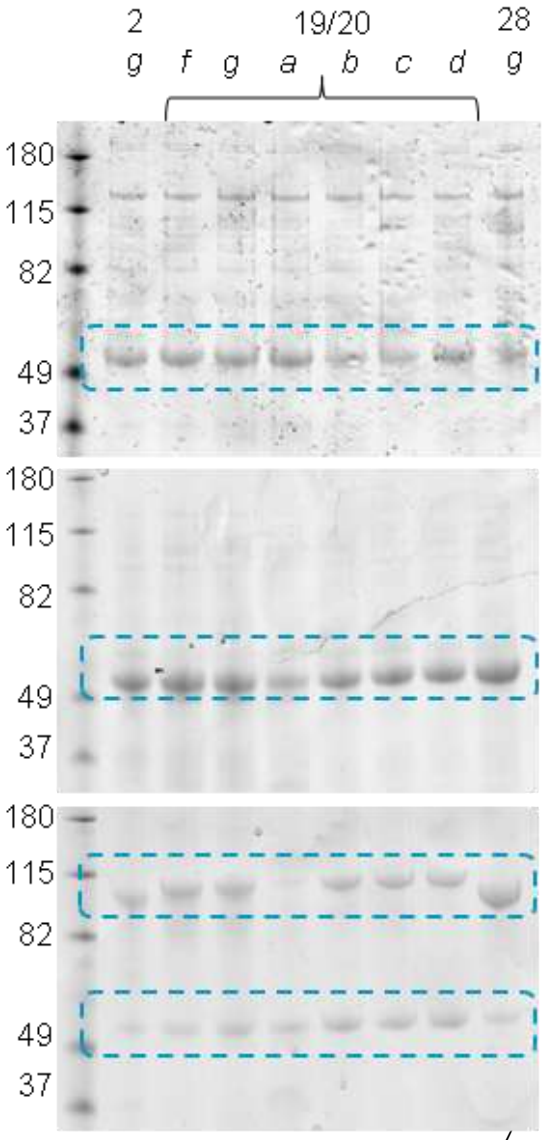

Figure 3. SDS-PAGE gel analysis of AmelF3 Ala-Cys mutations. (top) cell pellets from recombinant *E. coli* expressing various AmelF3 mutants under reducing conditions, (middle) AmelF3 mutants after purification under reducing conditions, (bottom) AmelF3 mutants after purification under non-reducing conditions. The position of the mutants is indicated at the top of the gel with number corresponding to heptad position and letters referring to position within the heptad. Numbers on

left indicate size of protein markers. The blue line surrounds expressed silk proteins.

Objective 3 - Verification of surface location of cysteine residues: *The purified silk protein mutants will be prepared under conditions that promote the formation of coiled coils. The amount of solvent exposed cysteine will be assessed by reaction with Ellmans reagent (5,5'-dithiobis(2-nitrobenzoate; DTNB). The product of this reaction is readily detected colorimetrically using a standard spectrophotometer.*

The mutated AmelF3 proteins described above were prepared under reducing conditions to break existing intermolecular disulfide linkages. After the reducing agent was removed the amount of solvent exposed cysteine was assessed colorimetrically using a standard spectrophotometer after reaction with Ellmans reagent (Table 2). The amount of Ellmans bound to cysteine (as percent of total number of cysteine residues present) was, as expected, highest for proteins mutated in non-core positions and lowest for proteins mutated in core positions.

Table 2. Detection of reactive cysteine residues on surface of mutated protein structures.

Position of mutation	Core or non-core position	% surface residues*
A196C	Non-core	92
A197C	Non-core	88
A198C	Core	49

*Calculated as percent of residues that were available to bind Ellmans reagent.

Modified Objective 4 – Determination of factors controlling artificial silk protein folding into native structure. *The effect of SDS and salt on folding AmelF3 in solution will be examined by circular dichroism (CD) to confirm factors that promote folding of the protein into the coiled coil structure.*

Recombinant bee silk proteins expressed and purified from the soluble fraction in *E. coli* do not fold into coiled coils and contain only around 10% α-helical structure (Shi et al., 2008). In contrast, recombinant silk proteins purified from *E. coli* inclusion bodies with the detergent SDS and refolded by reducing detergent levels, are predominantly coiled coil (see Objective 1). We prepared recombinant honeybee proteins without detergent and the CD spectra indicated that the proteins were predominantly random coil, in agreement with previous studies (Shi et al., 2008).

In an alternative method used to prepare proteins for functional assays and the synthesis of solid materials, recombinant proteins are isolated from the inclusion bodies and exposed to high salt levels and then to reduced SDS levels, both conditions under which protein oligomerisation is expected to be affected. SDS is known to disrupt tertiary structure and promote alpha-helical structure, while salt is known to stabilise coiled coils against urea and thermal denaturation by enhancing hydrophobic effects and thereby strengthening core interactions.

When SDS was added to above in concentrations above its critical micelle concentration (CMC), the proteins folded into predominantly an α-helical structure (Figure 4) with the observed protein

particle size consistent with monomeric (unassociated) helices (Table 3). Coiled coil α-helices are amphipathic, containing a stripe of hydrophobic residues along the helices that serve to drive coiled coil formation. Given the amphipathic nature of the helices, they are not expected to exist in solution in isolation. Therefore, SDS is stabilising the protein in the helical structure, presumably by shielding the hydrophobic 'core' residues from the solvent. We used molecular dynamics simulations to further explain the role of SDS in stabilising the secondary structure. The simulations were performed in an explicit water box (both with and without SDS), using a 9-heptad section of the silk that is predicted (with a high degree of confidence) to have helical secondary structure. Dynamics were performed on 10-20 ns timescales using the AMBER FF99SB forcefield. The simulations demonstrated SDS was stabilising the protein in an alpha helix conformation (Figure 5 and 6).

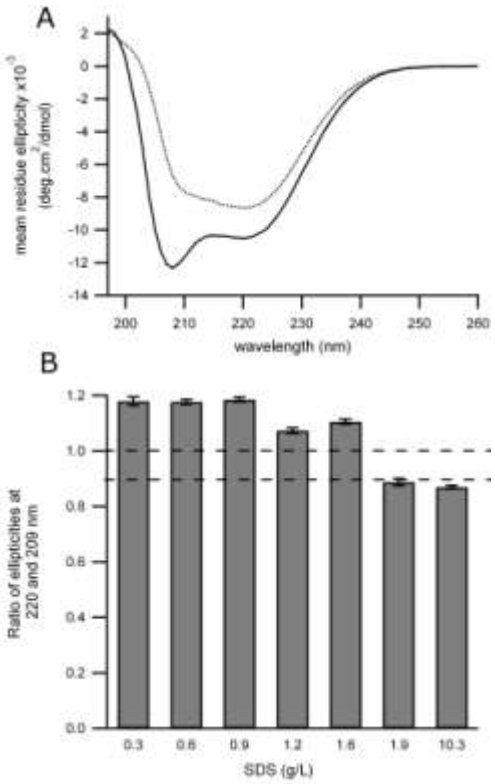

Figure 4. Effect of SDS on recombinant honeybee silk protein structure at 0.1 g/L salt concentration. A: Representative spectra of protein solutions in the presence of high (10.3 g/L; solid line) and low (0.3 g/L; dotted line) SDS concentrations B: Bars represent ratios of ellipticity at 220 nm and 209 nm, with ratios above 1 indicating coiled coil structure and ratios below 0.9 indicating non-interacting α-helices (Zhou, 1994). Error bars are the standard deviation of four measurements.

Table 3. Helix conformation and particle size of 4.1 g/L honeybee silk protein solutions at different SDS ratios and salt conditions.

SDS (g/L)	NaCl (g/L)	Predicted α-helix association[a]	Dominant particle diameter[b] (nm)
0.3	0.1	Coiled coil	10.3 ± 0.8
10.3	0.1	Dissociated	5.1 ± 0.04
0.3	14.1	Coiled coil	58.4 ± 3.9
10.3	14.1	Coiled coil	36.2 ± 8.5

[a]Determined from ratio of CD 220/209, with ratio above 1 indicating coiled coil and ratio below 0.9 indicating non-interacting α-helices (see Figure 1 and 2).
[b]average and standard deviation from six measurements.

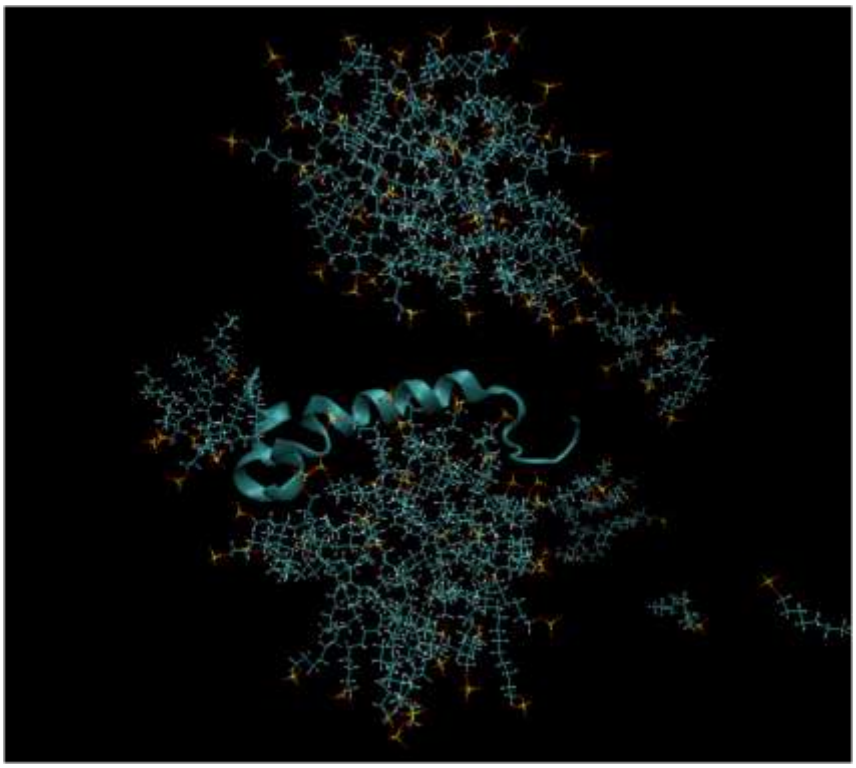

Figure 5. Molecular dynamics simulation of the α-helical structure of honeybee silk protein in the presence of SDS.

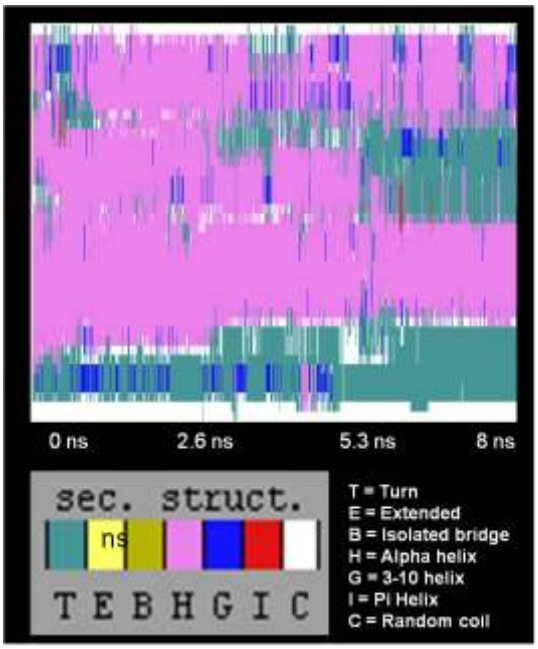

Figure 5. Protein predicted structural content during molecular dynamics simulation of the α-helical structure of honeybee silk protein in the presence of SDS.

In order to investigate the affect of salt on the formation and stabilisation of coiled coils, we added NaCl to the protein solutions containing low SDS (coiled coil proteins) and high SDS (unassociated α-helical structured proteins). The addition of NaCl reduces the predicted CMC of SDS but does not affect the solubility of the detergent, allowing SDS to remain and interact with the protein. At low detergent concentrations, addition of salt (14.1 g/L NaCl) did not affect the protein structure and it remained predominantly coiled coil (Figure 7). However, the protein particle size increased dramatically (Table 3). Aggregation of the coiled coils was not surprising, as salt out-competes the protein for water binding and hence drives the formation of protein-protein hydrogen bonds.

Addition of salt to the silk proteins in high SDS (α-helical structured) drove the formation of coiled coils (Figure 7) and an increase in the size of the protein particles (Table 3) indicating that the stabilising effect of salt on coiled coils exceeded the destabilising effect of micellular SDS. The size of the particles in the high SDS, high salt solutions were significantly smaller than the particles in low SDS, high salt conditions (Table 3). Normally salt would be expected to lead to an increase in protein-SDS particle size because salt shields electrostatic repulsion between the charged groups of the detergent molecules, allowing the molecules to pack more efficiently. The decrease in particle size observed in the presence of high SDS concentrations (Table 3) indicates that although SDS did not prevent protein-protein bonding within the coiled coil it did reduce inter coiled coil interactions.

Salt stabilises protein-protein, protein-SDS, and SDS-SDS interactions, all three by similar mechanisms but to different extents. Due to the interplay between these effects, at high SDS-to-protein ratios and low salt concentrations, interactions between SDS and protein are preferred, resulting in SDS-coated monomeric proteins (Figure 7 and Table 3). However, at high salt

concentrations protein-protein association is favoured, resulting in proteins assembling into coiled coils which then further aggregate (Figure 7 and Table 3). High concentrations of SDS are sufficient to partially disrupt the aggregates but not the coiled coils. Figure 8 summarises the relationships of these interactions. Recombinant silk proteins have not been assembled into coiled coils to date without SDS (Shi, 2008; our data). The method developed in our laboratory allows α-helical structure to be induced in recombinant proteins using SDS, and coiled coil formation to be induced from this intermediate structure using high salt concentrations. After reducing the concentration of SDS and salt to minor components, silk proteins remain in the native coiled coil conformation.

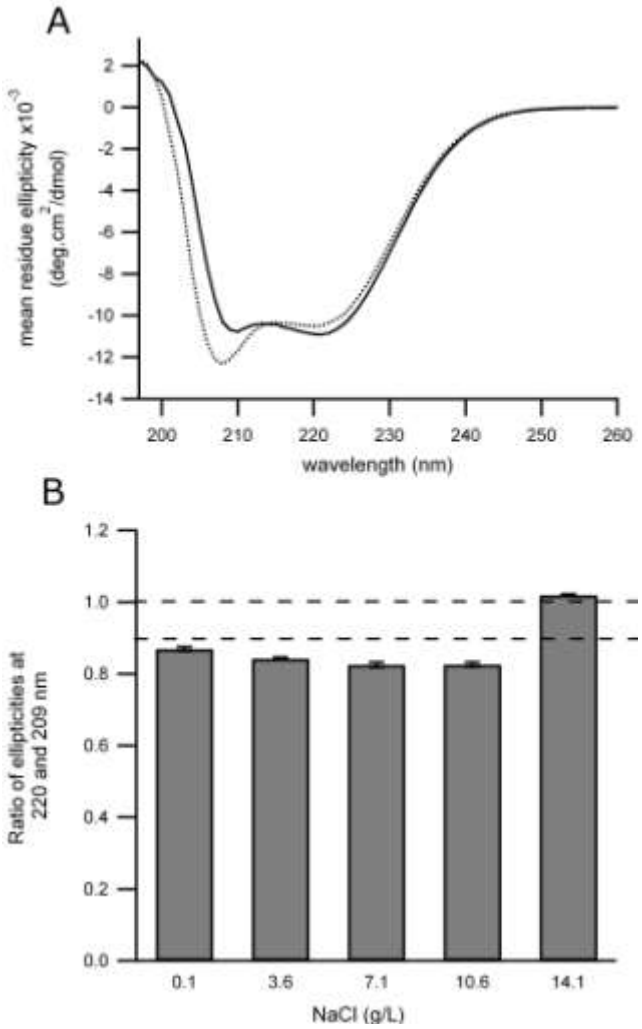

Figure 7. Effect of increasing salt concentrations on molecular structure of recombinant honeybee silk protein structure in the presence of 10.3 g/L SDS. A: Representative spectra of protein solutions in the presence of high SDS (10.3 g/L) and low (0.1 g/L; dotted line) and high (14.1 g/L; solid line) salt concentrations. B: Bars represent ratios of CD ellipticity at 220 nm and 209 nm, with ratios above 1 indicating coiled coil structure and ratios below 0.9 indicating non-interacting α-helices (Zhou et al., 1994). Error bars are the standard deviation of four measurements.

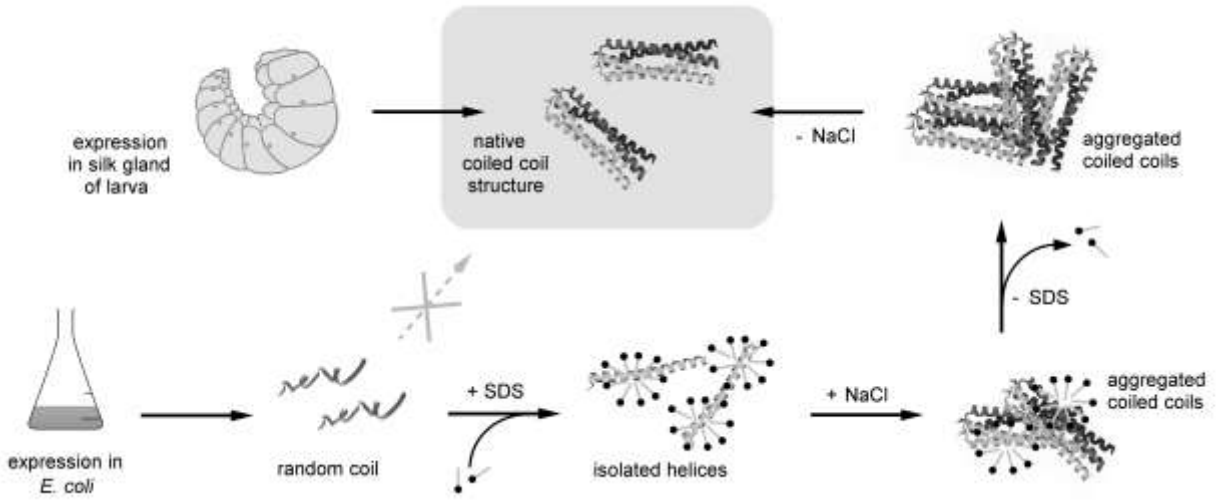

Figure 8. Schematic of honeybee silk protein folding pathways.

Objective 5 - Synthesis of silken materials: *Mutant silk proteins will be concentrated by dialysis against commercially available protein concentrating reagents. Concentrated silk protein solutions will be fabricated into fibres by extrusion into a methanol coagulation bath, dried and then drawn to 100% their original length or by electrospinning.*

Silken fibres were prepared as described in Sutherland et al. (2011). Furthermore, two methods were developed to generate high surface area, low volume materials: electrospun fibres and freeze-dried sponges (Figure 9). Each new material type is described in detail below.

Fabrication of protein solutions into nanoscale fibres. Honeybee silk protein AmelF3 was expressed into the inclusion bodies of *E. coli*, the inclusion bodies purified using BugBuster Master Mix (Novagen) according to the manufacturer's protocol and then the silk protein solubilised in 3% sodium dodecyl sulfate (SDS) with 2 h incubation at 60°C. Detergent was removed after addition of KCl (300 mM final) caused precipitation of potassium dodecyl sulfate (KDS). KDS was removed by centrifugation at 16 000 *g* for 5 min and the solution was dialysed against 20% PEG 8000 until the protein concentration reached 12.5%. Silk/polyethylene oxide (PEO) blends were prepared by adding the required amount of 5.0% (wt/vol) PEO (900 000 MW, Sigma) into the silk solution and then gently stirring for 20 min. The silk/PEO solution was delivered through a 16G stainless steel capillary maintained at high electric potential at a flow rate of 0.005 – 0.01 ml/min using a Sage syringe pump (Thermo Scientific). The collector was a grounded aluminum foil placed on a 10 cm diameter aluminum plate. Silk was collected directly on the aluminum foil except for the cell study, where it was collected on 9x9 mm^2 glass

coverslips that were placed on the top of the usual aluminum foil. Electrospinning was conducted at room temperature (20–22˚C) and humidity levels of 16–17%. Honeybee silk protein solutions alone did not electospin at the concentration tested (12.5% protein w/v) and was required to be blended with PEO at 0.67 or 1% before fibres could be spun. Electrospinning generated fibres of 200 nm (Figure 9A).

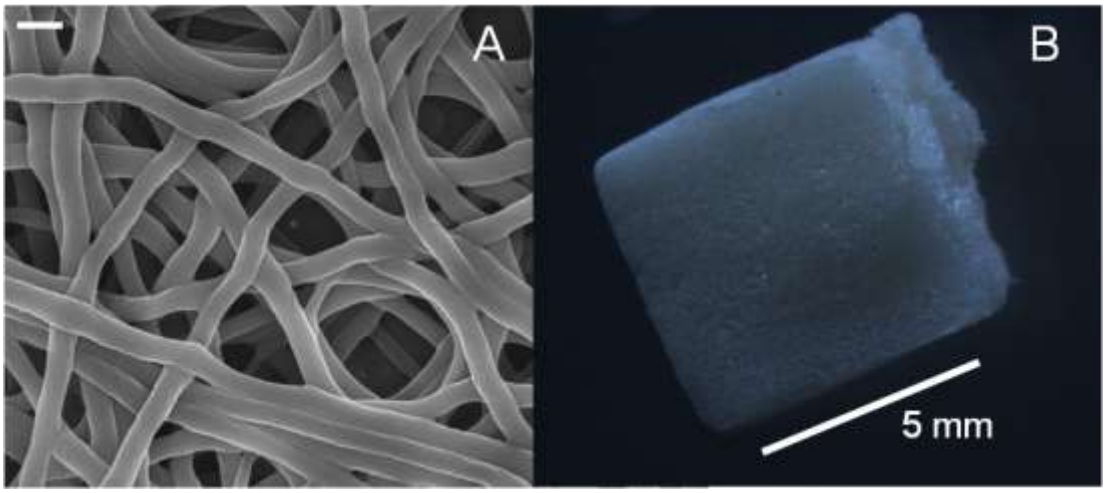

Figure 9. High surface area materials generated from recombinant honeybee silk proteins. (A) Electrospun fibres, scale bar is 200 nm. (B) Freeze dried sponges.

Fabrication of protein solutions into sponges. Honeybee silk protein was expressed as described above. The final protein solution was poured into silicone rubber moulds (14 x 5 x 6 mm; RL060, ProSciTech, QLD), frozen at -20ºC overnight, and placed in a freeze-dryer (FD355DMP, FTS Systems) for 24 hours to generate sponges (Figure 9B).

Objective 6 - Proof-of-concept functionalisation: *The availability of reactive cysteine on the surface of the silk thread will be assessed by reaction with a fluorophore such as 5-iodoacetamidofluorescein (5-IAF) and examination of the threads by fluorescence microscopy.*

Whilst the fluorophore 5-IAF could be bound to the cysteine residues on the surface of fibres generated from AtoC mutant proteins and then detected by fluorescence microscopy (Figure 10A), non-specific binding was also seen on threads generated from control proteins (Figure 10B). A quantitative experiment was undertaken to determine the extent to which 5-IAF binds non-specifically to AmelF3 fibres. Electrospun mats were immersed in 5-IAF solutions and the changes in 5-IAF concentrations were determined. Figure 10C shows the relationship between initial fluorescein concentrations used and the amount of fluorescein which bound to the protein fibres. Extensive washing of the electrospun mats after 5-IAF binding removed only a small proportion of the fluorescein. When electrospun mats were treated with solutions of very low fluorescein concentration, the degree of binding stabilized at approximately 0.05 moles of fluorescein per mole of protein. This is equivalent to approximately three molecules of fluorescein bound non-specifically to each molecule of protein located on the surface of the fibres. For comparison, AmelF3 proteins with a single point mutation are capable of specifically

binding up to one molecule of fluorescein per surface protein. Since non-specific binding is threefold greater in magnitude than the specific binding, we conclude that it is not possible to achieve controlled functionalization by specific binding using this method. We note that high levels of non-specific binding to silkworm silk have been reported in other laboratories (Lammel et al., 2011).

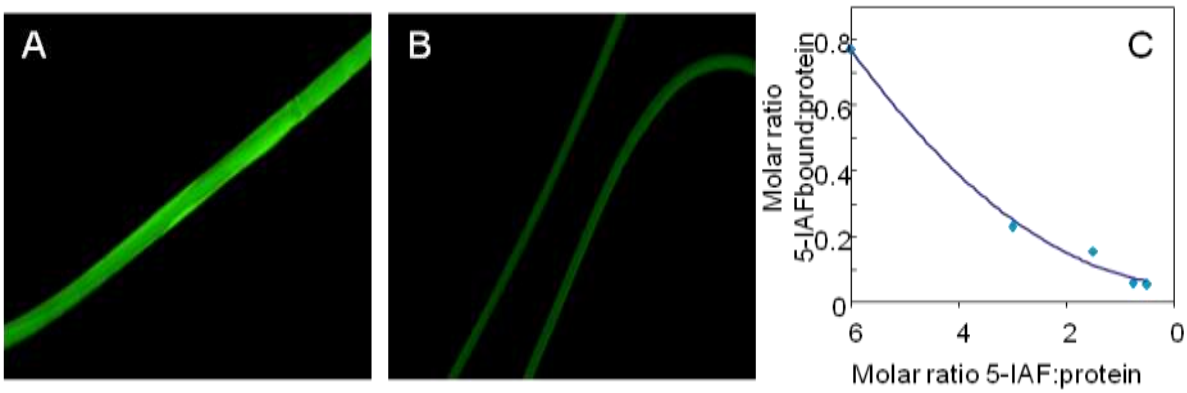

Figure 10. Assesment of the availability of reactive cysteines on the surface of the silk thread as assessed by reaction with a fluorophore. (A) Fluorescence micrograph of mutant (A) and control (B) AmelF3 protein fibres stained with a cysteine-reactive fluorophore (IAF). (C) Graph showing binding of 5-IAF solutions to AmelF3 electrospun mats.

Objective 7 - Physical analysis of functionalised fibres: *The tensile strength and extensibility of the functionalised fibres will be measured using an Instron Tensile tester to assess the effects of the mutagenesis on the native properties of the material.*

The strength and elasticity of the mutant proteins were indistinguishable from that of fibres generated from non-mutated proteins (of equivalent diameter).

Objective 8 – Recursion: *If the above steps do not produce the desired results, we will refine the structural model and select alternate sites for mutagenesis.*

Objective 8 findings: Refining the structural model: evidence for different types of cross-links in different coiled coil silk lineages. At the onset of this project, the model for the molecular structure of silk from the Hymenopteran superfamilies Apoidea (honeybee) and Vespoidea (ants/hornets) was that of aligned coiled coil proteins. The model was based on early X-ray fibre diffraction data demonstrated that silk fibres drawn from honeybee silk glands contained α-helical proteins assembled into a coiled coil structure (Rudall, 1962,1965; Atkins, 1967).

During the period of this grant, we investigated different types of cross-linking in the coiled coil silks. Two post-spinning treatments were used to generate varying levels of ß-sheet in electrospun recombinant honeybee fibers: water annealing and methanol treatment. Both methods are commonly used to induce ß-sheet formation in reconstituted silkworm silk and

result in water insensitive material. FTIR analysis demonstrated that the molecular structure of the fibers after both methanol and water annealing treatments lead to an increased spectral peak at 1626 cm^{-1}, indicating an increase in ß-sheet content in the silk proteins (Figures 11B-H). Water annealing led to a gradual increase in ß-sheet content over at least 16 hrs (Figure 11B-G) whereas 10 minute methanol treatment had a rapid greater impact on the ß-sheet content (Figure 11H). Only fibres with significant levels of ß-sheet content were water insoluble. From these results we were able to correlate the mechanical performance and water stability of artificial honeybee silk material with the ß-sheet content of the material.

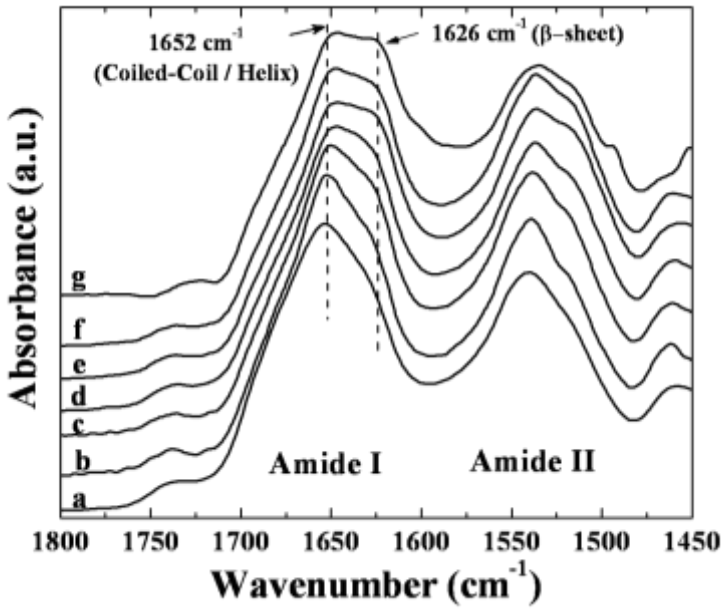

Figure 11. Fourier transformed infrared (FTIR) spectra of the amide I and II regions of electrospun honeybee silk before and after treatments to make the fibers water insensitive. As spun fibers (A), after water annealing for 7 min (B), 15 min (C), 30 min (D), 60 min (E), 120 min (F), overnight (G); and after methanol treatment (H). Assignments of bands to structures are described in the text.

We analysed X-ray diffraction patterns from weaver ant (Vespoidea) silk and honeybee (Apoidea) silk. The plots demonstrated that scattering observed from the silk from bees is dominated by the coiled coil signal, while the scattering from silk from the ants contains both coiled coil and ß-sheet signals with comparable intensity (Figure 12). Previously we had demonstrated that honeybee silk is particularly intractable to chemical agents generally used to solubilise silk and more resistant to solubilisation than ant/hornet silk (Sutherland et al., 2006). The ß-sheet content of native honeybee silk did not correlate to the physical properties of the material and does not agree with the above model for artificial honeybee silk. In contrast, hornet silk (Vespoidea) can be solubilised in lithium bromide (akin to silkworm silk). Therefore, the structure and physical properties of Vespoidea silk is consistent with our refined model where coiled coils are cross-linked by ß-sheet structures.

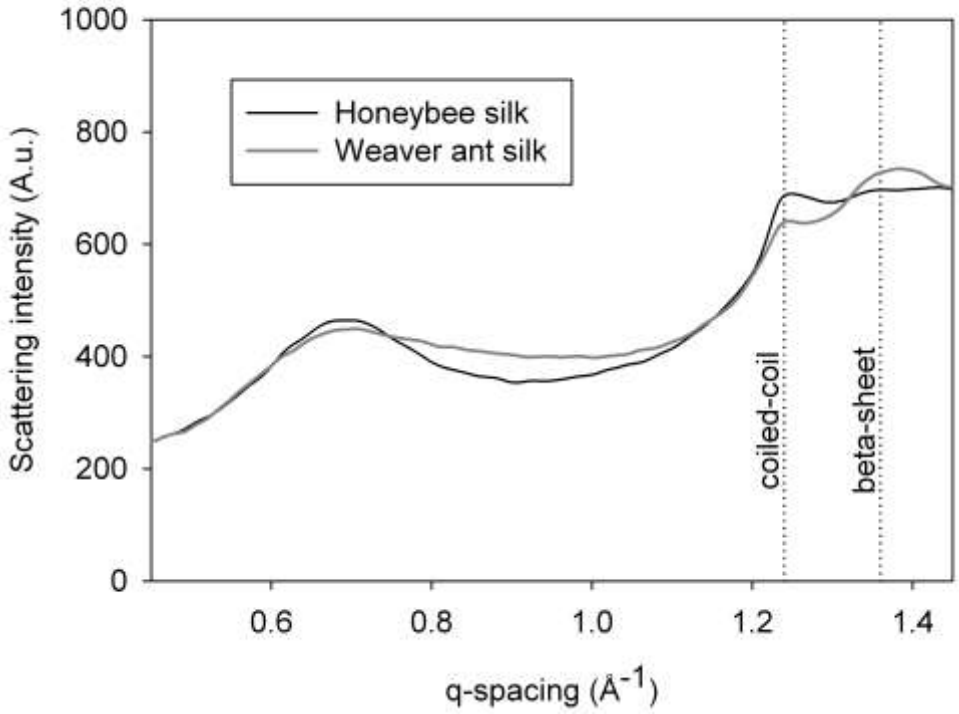

Figure 12. Comparison of WAXS plots of native honeybee and of weaver ant silk sheets, examined under identical experimental conditions.

Refining the structural model: nature of cross-links in native honeybee silk. We conducted a range of experiments aimed at discovering the nature of protein cross-linking between the native honeybee proteins. The experiments and findings are described in detail below and in summary are:

1. Amino acid analysis of native honeybee silk found that the measured level of lysine was significantly less than the level predicted from the protein composition. Lysine cross-links would prevent detection of lysine and therefore this result implying the presence of lysine cross-links.
2. Silk proteins isolated from the silk gland do not run as monomers on SDS-PAGE, implying that the proteins are cross-linked in the silk gland.

Amino acid analysis of native silk: We used acid hydrolysis to determine relative amino acid composition of native honeybee silk and compared the experimentally derived results to the levels of amino acids predicted from the known protein composition (Figure 13). From this analysis we detected a discrepancy between measured and calculated Lys content. It should be noted that, given that Ala-Ala bonds are particularly difficult to hydrolyse using acid hydrolysis, the measured composition is expected to underestimate the Ala content hence the relative

amount of other amino acids is expected to be overestimated. This analysis suggests that lysine cross-links may be present in native honeybee silk.

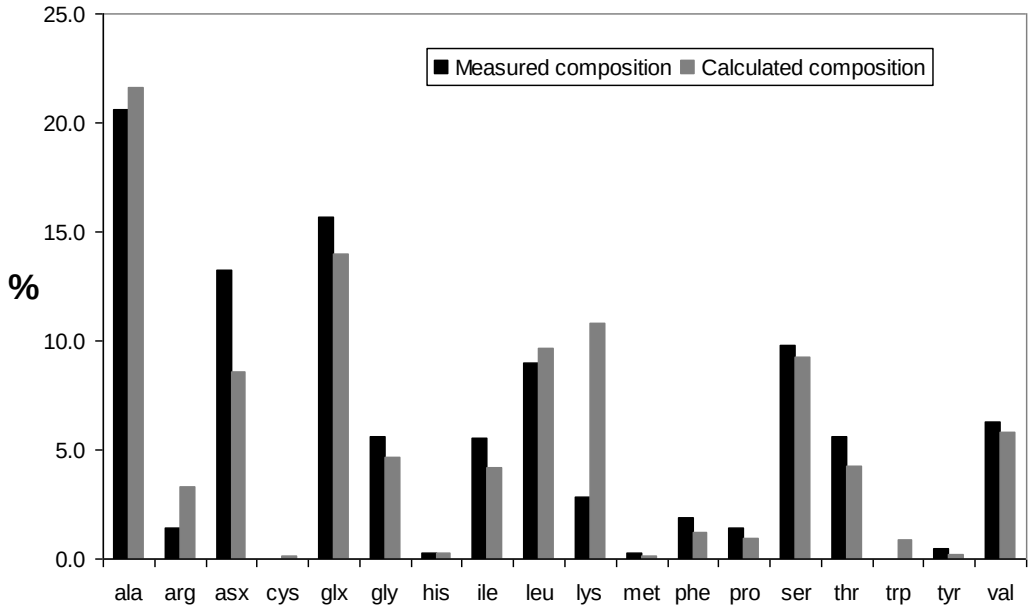

Figure 13. Comparison of measured amino acid composition to composition calculated from silk protein composition.

SDS-PAGE analysis of native silk proteins from silk gland: Given that honeybee silk has, to date, proven intractable to solubilisation in any chemical reagents, we analysed the silk proteins from the silk glands. We isolated silk proteins from the silk glands of honey bees and ran them on SDS-PAGE gels and analysed the banding pattern of silk proteins using LC/MS (Figure 14). We found, in addition to proteins migrating as expected for monomers, the proteins migrated as expected for multimeric proteins. It is generally expected that proteins will be resolved as monomers on SDS-PAGE unless they are covalently cross-linked for example by disulfide bonds. The honeybee silk proteins do not contain any cysteine residues and therefore cannot form thiol cross-links. The banding pattern on SDS-PAGE suggests that the native honeybee silk proteins are covalently cross-linked in the gland prior to spinning.

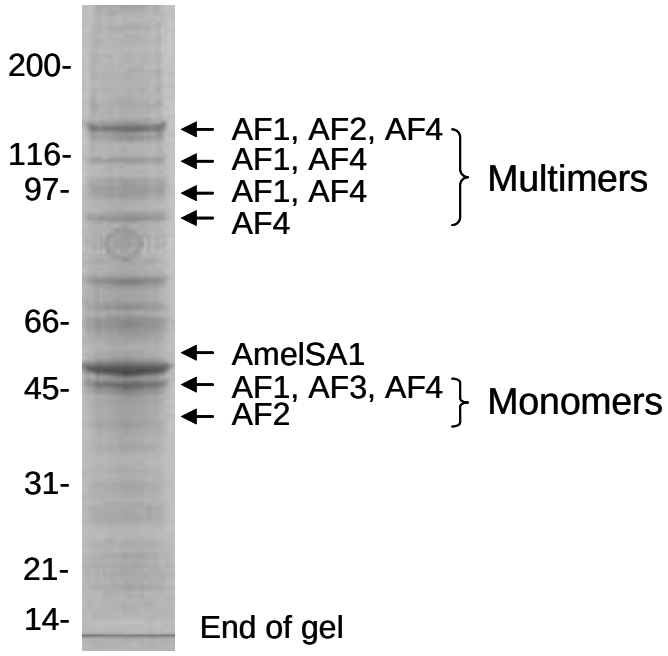

Figure 14. Native honeybee silk proteins (AF1-4; AmelSA1) isolated from silk gland and run on SDS PAGE. The expected size of the monomer proteins is indicated. The presence of monomers of the AF1-4 proteins is also indicated.

Refining the structural model: mimicking covalent cross-linking in artificial honeybee silk materials. We developed two methods to covalently cross-link artificial honeybee proteins without the addition of chemical cross-linking reagents: heat treatment and transglutaminase. Both treatments lead to the material becoming stable in protein denaturants such as urea, guanadinium and SDS. We examined the material by FTIR and found that the secondary structure of the proteins had not changed structure significantly.

Amino acid analysis was performed on acid hydrolysed control and heat treated sponges and results are shown that heat treatment resulted in losses in lysine (21.5 mg/g sponge, ~6 lysine residues per protein) and serine (8.9 mg/g sponge, ~ 4 serine residues per protein), although due to the level of serine in the material the loss of serine is not as convincing as the loss of lysine. Serine and lysine residues are known to form lysinoalanine cross-links in other proteins subjected to heat treatment through dehydration of the serine to form a dehydroalanine electrophile which can then undergo nucleophilic attack by the lysine's primary amine. The analogous reaction with threonine, which also exhibits a significant reduction, is known to occur, forming methyl-lysinoalanine. Raman bands associated with the symmetric C-N-C stretching vibrations of lysinoalanine and methyl lysinoalanine are expected in the 850 to 900 cm^{-1} region which is already rich in protein skeletal vibrations. However, no significant spectral changes were observed in this region as a function of thermal treatment.

Heat treatment will also generate isopeptide bonds or esters between amine-functional, or potentially amine-functional sidechains (Lys, Arg, His, Asn, Gln), and acidic residues such as Asp and Glu in close proximity. Isopeptide and ester bonds cannot be inferred from the amino acid analysis as acid hydrolysis will hydrolyse all amide and ester bonds, returning the original amine, hydroxyl and carboxylate functional groups, except in the case where Arg could be thermally converted to a primary amine and form isopeptide bonds. In this event, hydrolysis would, of course, only return the primary amine. Indeed, there does appear to be a slight reduction in Arg content upon heat treatment at 190 ^{o}C for 60 min which may be indicative of this manner of crosslinking having occurred. Isopeptide bonds are difficult to observe directly in Raman spectra owing to their relatively low abundance compared to the backbone amides, which will absorb in the same region. While the carbonyl stretching vibrations of ester groups are expected on the high frequency side of the amide I band, its weak intensity in the Raman compared to that in the infrared making it hard to detect at low concentrations. Therefore, to measure the contribution of isopeptide and ester bonds to the heat treated materials properties, we conducted amino acid analysis was performed on enzymatically hydrolysed control and heat treated (60 min at 190°C) sponges. The enzymatically hydrolysed heat treated material showed significant losses in lysine (33.9 mg/g, ~9 lysine residues per protein), asparagine (7.0 mg/g, ~2 asparagine residues per protein), glutamate (12.5 mg/g, ~ 4 glutamate residues per protein) and aspartate (15.4 mg/g sponge, ~ 4 aspartate residues per protein) in comparison to the unheat treated sponges. The presence of ε-(γ-glutamyl)-lysine in heat treated scaffolds was confirmed using LCMS. The dipeptide was not detected in non-heat treated scaffold materials. These results indicate that the heat treatment is generating isopeptide bond formation between lysine or aspargine and glutamate or aspartate.

Transglutaminase will generate an isopeptide bond between lysine and glutamine and therefore, after transglutaminase treatment, the observed frequency of these amino acids would be expected to decrease. As expected, the transglutaminase treated material was deficient in lysine (8.5 mg/g, ~2 lysine residues per protein), glutamine (5.2 mg/g, ~ 2 glutamate residues per protein).

These results indicate two important findings:

a) Lysine residues are positioned in the material so that they can react with either aspartate and glutamate residues or with glutamine residues.
b) Formation of covalent cross-links through these materials generates chemically stable materials akin to native materials.

Supported Personnel

The project was initially co-funded 50% by CSIRO. However, changes in the value of the Australian dollar relative to the US dollar have altered the funding ratio so that now the project is co-funded around 75% by CSIRO. The staff allocated to the project are:
Tara Sutherland (PI, 20%)
Alagacone Sriskantha (Post PhD, 100%)
Micky Huson (Senior Research Scientist, 5%)

Collaborations

1. David Kaplan, TUFTS University. We are collaborating with David around developing biomaterials from honeybee silk. In 2010, David hosted a four week visit by the PI of this project. The PI then hosted a visit of three months of one of David's postdoctoral fellows. Three shorter inter-laboratory visits have also occurred. Of specific relevance to this project is the development of electrospun fibre mats. Electrospun honeybee fibres have a diameter of 200 nm. The enormous surface area of these mats in comparison to the surface area of wet-spun fibres is ideal for measuring the efficiency of modifications to the surface of silk fibres.

2. Fritz Vollrath, Oxford. We are collaborating with Fritz around silk rheology. In 2010, Fritz hosted a three week visit by the PI of this project. This work is ongoing.

3. Dimitri Deheyn, SCRIPPS. We have provided Dimitri with numerous silk samples for analysis.

4. Tsunenori Kameda, NIAS. We collaborate with Tsun on silk structure analysis, particularly solid state NMR analysis of native and artificial materials.

5. Other CSIRO scientists. We have a strong collaboration with a number of CSIRO scientists across a number of sites. Of particular relevance are collaborations with Dr Jeff Church (infra red analysis), Dr Jacinta Poole (material science), Dr Sarah Weisman (silk structure function analysis), Dr Andrew Warden (molecular dynamics simulations).

Publications

1. Wittmer CR, Hu H, Gauthier P-C, Weisman S, Kaplan DL, Sutherland TD. 2011. Production, structure and *in vitro* degradation of electrospun honeybee silk nanofibres. *Acta Biomaterialia*, 7:3789-3795.

2. Sutherland TD, Jeffrey S. Church JS, Hu X, Huson MG, Kaplan DL, Weisman S. 2011. Single honeybee silk protein mimics properties of multi-protein silk. *PLoS ONE* 6(2): e16489. doi:10.1371/journal.pone.0016489.

3. Walker AA, Weisman S, Sutherland TD. Control of coiled coil protein folding using SDS and salt (submitted to Macromolecules).

4. Huson MG, Church JS, Poole JM, Weisman S, Sriskantha S, Warden AC, Ramshaw JAM, Sutherland TD. Structural and physical changes of honeybee silk materials induced by heating or by immersion in aqueous methanol solutions. (submitted to PLoS One)

Interactions/Transitions

Transitions: We are working with Lonza to develop large scale recombinant production of honeybee silk proteins for a range of applications.

Interactions: Dimitri Deheyn, Scripps Institute of Oceanography. We have provided Dimitri with a range of silk samples containing different molecular structures for analysis of their optical properties.

References mentioned in report

Heimburg T, Schünemann J, Weber K, Geisler N (1999) FTIR-spectroscopy of multistranded coiled coil proteins. *Biochemistry* 38:12727-12734

Hepburn HR, Chandler HD, Davidoff MR (1979) Extensometric properties of insect fibroins: the green lacewing cross-ß, honeybee α-helical and greater waxmoth parallel-ß conformations. *Insect Biochem* 9:69-77.

Lammel A, Schwab M, Hofer M, Winter G, Scheibel T. 2011. Recombinant spider silk particles as drug delivery vehicles. Biomaterials 32:2233-2240

Shi J, Lua S, Du N, Liu X, Song J (2008) Identification, recombinant production and structural characterization of four silk proteins from the Asiatic honeybee *Apis cerana*. Biomaterials 29:2820-8

Sutherland TD, Campbell PM, Weisman S, Trueman HE, Sriskantha A, Wanjura WJ, Haritos VS (2006) A highly divergent gene cluster in honey bees encodes a novel silk family. *Genome Res*. 16:1414-21.

Sutherland TD, Jeffrey S. Church JS, Hu X, Huson MG, Kaplan DL, Weisman S. (2011) Single honeybee silk protein mimics properties of multi-protein silk. *PLoS ONE* 6(2): e16489. doi:10.1371/journal.pone.0016489.

Zhou NE, Kay CM, Hodges RS (1994) The net energetic contribution of interhelical electrostatic attractions to coiled-coil stability. *Protein Eng* **7**:1365–1372.